8-2016

Assessing the feasibility of a one-pot, tandem olefin metathesis and isomerization sequence to synthesize conjugated aromatic olefins

Ajay D. Makwana
University of Tennessee at Chattanooga, whj271@mocs.utc.edu

Assessing the Feasibility of a One-Pot, Tandem Olefin Metathesis and Isomerization Sequence to Synthesize Conjugated Aromatic Olefins

Ajay D. Makwana

Departmental Honors Thesis
The University of Tennessee at Chattanooga
Department of Chemistry

Project Director: Dr. Kyle S. Knight
Examination Date: April 4, 2016

Members of Examination Committee:
Dr. John P. Lee
Dr. Han J. Park
Dr. David Giles

Abstract

The synthesis of substituted phenylpropene dimers using a one-pot, tandem olefin metathesis and isomerization sequence has been studied. This sequence relies on the facilitated, *in-situ* conversion of a ruthenium carbene species (Ru=C) to a ruthenium hydride species (Ru-H) upon addition of an inorganic hydride source. Three separate reactions occur within one reaction flask: 1) olefin metathesis of the starting phenylpropene to yield phenylpropene dimer via Ru=C catalyst, 2) conversion of Ru=C to Ru-H via addition of an inorganic hydride source, 3) isomerization of phenylpropene dimer via insertion and β-hydride elimination to yield conjugated product.

The focus of the study has been to determine optimal reaction conditions to facilitate the formation of a high yield of dimerized product. Thus far, the isolation of the dimerized product has been elusive due to the thermodynamically favorable formation of the isomerized dimer product. The isomerized dimer has been observed to undergo further olefin metathesis via the action of residual Ru=C catalyst resulting in the formation of several metathesis alkene products. A variety of metathesis products in the crude reaction mixture has been consistently detected via ^{1}H NMR spectroscopy under a range of experimental conditions.

Table of Contents

List of Tables

List of Figures

Introduction

Recent advancements in chemical synthesis have been fundamental in expanding novel research in the biological sciences, pharmaceutical industry, and materials science. In particular, the synthesis of natural product analogues has been vital to the discovery and development of new drugs. In order to demonstrate the influence of organic chemistry in drug design, an analysis of the sources of new drugs from 1981-2010 indicated that 40% of new chemical entities were discovered with inspiration from a natural product.[1] To keep up with the growing demands of rapidly progressing scientific knowledge in the aforementioned disciplines, new categories of organic synthesis such as transition metal-catalyzed olefin metathesis reactions have been developed.[1, 2] The diverse applications of olefin metathesis reactions and their many side reactions have truly opened the door for the development of novel synthetic methods.

Purpose

The primary objective of this project was to assess the feasibility of a tandem olefin metathesis and isomerization sequence in order to synthesize conjugated aromatic olefins. Various phenylpropene compounds underwent homodimerization through olefin metathesis via action of the Grubbs Second Generation catalyst. Through an unknown mechanism, the Grubbs catalyst degraded from a ruthenium-carbene catalyst to a ruthenium-hydride catalyst and facilitated the double bond migration of the dimerized phenylpropene substrate resulting in conjugation with the aromatic ring.[14] Refining the reaction conditions for the greatest conversion of starting material to isomerized dimer posed the greatest challenge due to the undesired formation of several cross metathesis

side products. After synthesis, compounds were analyzed and characterized using thin layer chromatography (TLC), nuclear magnetic resonance (NMR) spectrometry, and X-ray diffraction crystallography when required. Successfully understanding each step of the tandem reaction and optimizing the formation of isomerized dimer may potentially lead to future research and applications in natural products synthesis.[29]

Olefin Cross Metathesis

Olefin metathesis is a class of synthetic techniques that facilitate the formation of highly functionalized olefin compounds from relatively simple alkene precursors. The general underlying mechanism behind olefin metathesis involves the rearrangement of the carbon atoms around two carbon-carbon double bonds through the action of a transition metal-based catalyst.[3] The three major types of olefin metathesis include ring-opening metathesis polymerizations (ROMP), ring-closing metathesis (RCM), and olefin cross metathesis (CM), with the latter being utilized in this research project.[4, 14] A general mechanism of CM is shown below in Figure 1 while a general catalytic cycle is shown in Figure 2 on the following page.[5] Of particular interest in Figure 2 is the exchange of R-substituents between the two alkene species via formation and action of the metallacyclobutane complex. In Figure 2, L represents an N-heterocyclic carbene ligand.

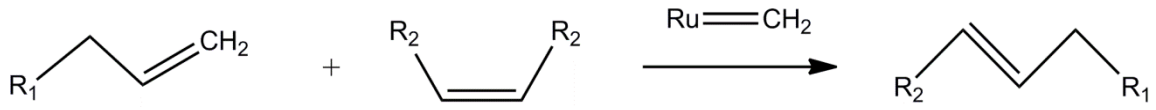

Figure 1: General Mechanism of Olefin Cross Metathesis

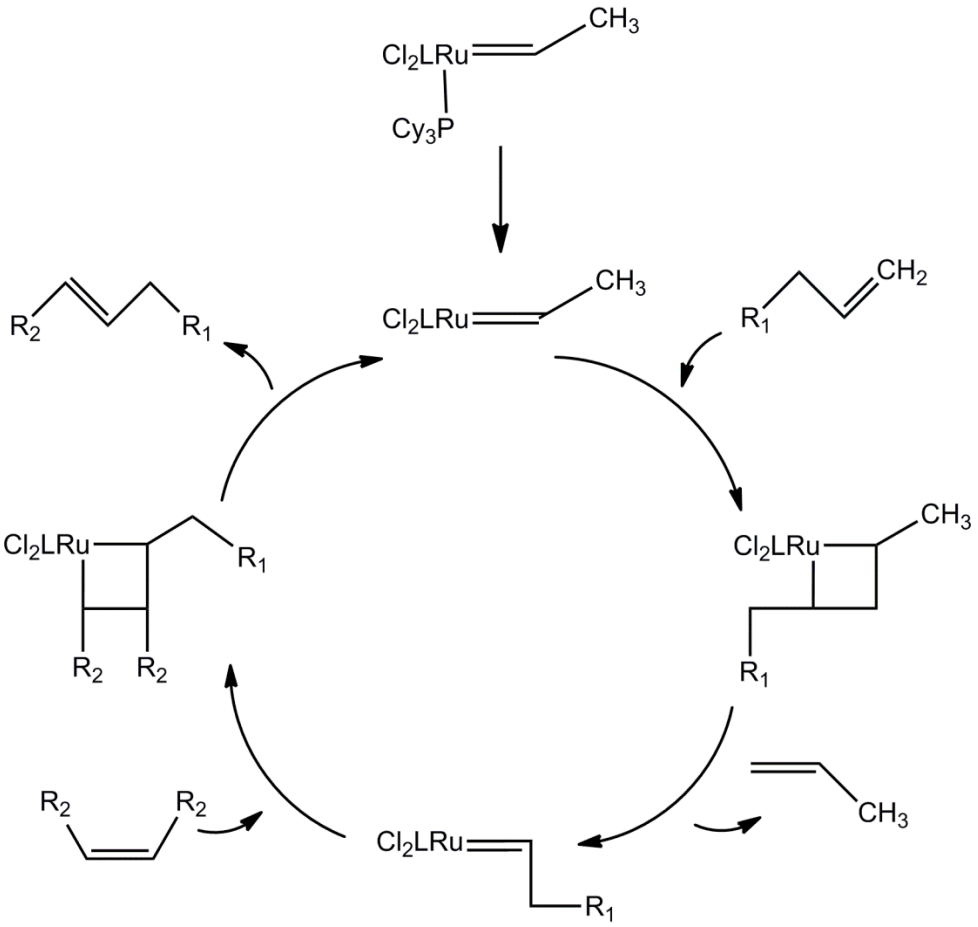

Figure 2: Olefin Cross Metathesis Catalytic Cycle

Although olefin cross metathesis is gaining popularity among organic chemists, there are some considerable disadvantages to the synthetic method including lack of predictability in product selectivity and stereoselectivity.[6] Furthermore, chemists have discovered that olefin compounds react differently during CM due to variations in functional groups, sterics, and electronic effects.[6] A general olefin classification scheme was developed by Chatterjee et al. that categorizes olefins based on their relative reactivity in CM, ranging from rapid homodimerization to no reactivity in CM.[6] This olefin classification scheme is detailed in Table 1 on the following page.

Table 1: Olefin Categories for Selective Cross Metathesis by Chatterjee et al.[6]

Olefin Type	Catalyst	Olefin Descriptions
Type 1 (fast homodimerization)	Grubbs 2nd Generation	terminal olefins, 1° allylic alcohols, esters, allyl boronate esters, allyl halides, styrenes (no large ortho substit.), allyl phosphonates, allyl silanes, allyl phosphine oxides, allyl sulfides, protected allyl amines
Type 2 (slow homodimerization)	Grubbs 2nd Generation	styrenes (large ortho substit.), acrylates, acrylamides, acrylic acid, acrolein, vinyl ketones, unprotected 3° alcohols, vinyl epoxides, 2° allylic alcohols, perfluorinated alkane olefins
Type 3 (no homodimerization)	Grubbs 2nd Generation	1,1-disubstituted olefins, non-bulky trisub. Olefins, vinyl phosphonates, phenyl vinyl sulfone, 4° allylic carbons (all alkyl substituents), 3° allylic alcohols (protected)
Type 4 (spectators to CM)	Grubbs 2nd Generation	vinyl nitro olefins, trisubstituted allyl alcohols (protected)

Grubbs Second Generation Catalyst

As interest in olefin metathesis increased and further applications for the synthetic technique emerged, great effort was focused on developing more efficient transition metal based metathesis catalysts.[7] Currently, several transition metal catalysts exist for olefin metathesis processes including ruthenium, molybdenum, titanium, and tungsten based catalysts.[6, 8] Among these, ruthenium and molybdenum catalysts have been the

most popular due to their high activity in olefin metathesis.[8, 9] Generally, molybdenum based catalysts are highly reactive towards a variety of olefin substrates, particularly when prepared and used in an inert atmosphere; however, poor functional group tolerance and high cost pose significant challenges for many research groups.[6-9] Ruthenium based catalysts, on the other hand, show little sensitivity to air, moisture, and slight solvent impurities as well as a high tolerance for organic functional groups such as aldehydes, carboxylic acids, and alcohols which have been demonstrated to render molybdenum catalysts inactive.[6, 31] The ruthenium based Grubbs second generation catalyst was used in this research project. The structure of the catalyst is shown below in Figure 3.

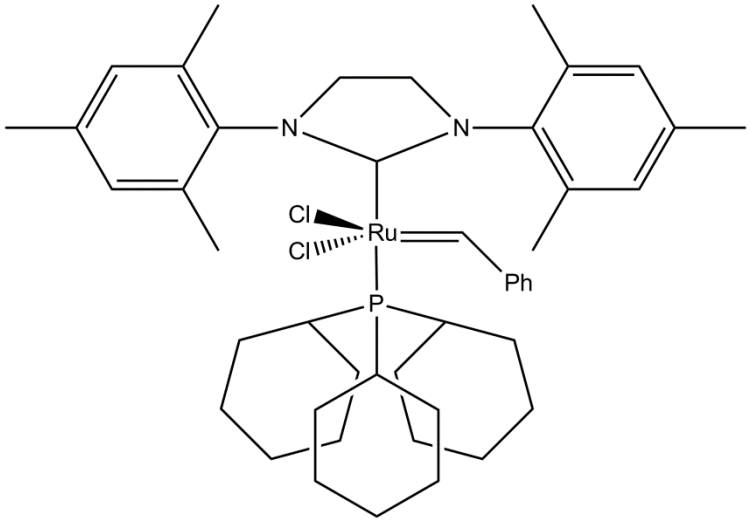

Figure 3: Structure of Grubbs Second Generation Catalyst

The primary site of metathesis activity in the Grubbs second generation catalyst is the nucleophilic Ru=C bond, also called the ruthenium carbene. Furthermore, the N-heterocyclic carbene ligand (NHC) acts to stabilize ruthenium intermediates in the catalytic cycle as it is a strong σ-donor.[10, 11] Despite its success, the Grubbs second generation catalyst, like other ruthenium based metathesis catalysts, has been observed to

decompose from its original ruthenium carbene state to a ruthenium hydride state during the course of a reaction.[12, 28, 30] The mechanism for this decomposition remains unknown, but ultimately results in the catalysis of undesired double bond migrations within the olefin starting materials.[30]

A suspension of catalyst in paraffin wax was prepared in order to maintain the potency of the catalyst.[13] Several literature sources indicate an increase in catalyst lifetime from approximately 30 days to over 22 months as a result of this preservation technique.[13] Although the paraffin wax does not interfere with the catalyst activity, additional measures must be taken to separate residual wax from the crude reaction mixture.

Olefin Isomerization

As mentioned previously, the decomposition of the Grubbs second generation catalyst results in the *in situ* formation of a ruthenium hydride species which catalyzes an olefin double bond migration reaction via insertion of the ruthenium hydride and subsequent β-hydride elimination in the olefin-metal hydride complex.[14, 22, 23] This phenomenon was first observed during early metathesis research and was further investigated by McGrath and Grubbs, who utilized deuterium labeling to conduct mechanistic studies, ultimately concluding that the isomerization occurred via a stereospecific *syn* 1,2-addition-elimination sequence of a transition metal hydride intermediate. The transition metal primarily attacked position two of the allyl group.[14, 25] Furthermore, this mechanism accounts for the high selectivity of *trans* product during

isomerization.[14, 25] A general mechanism for olefin isomerization via insertion and β-hydride elimination is shown in Figure 4 on the following page.

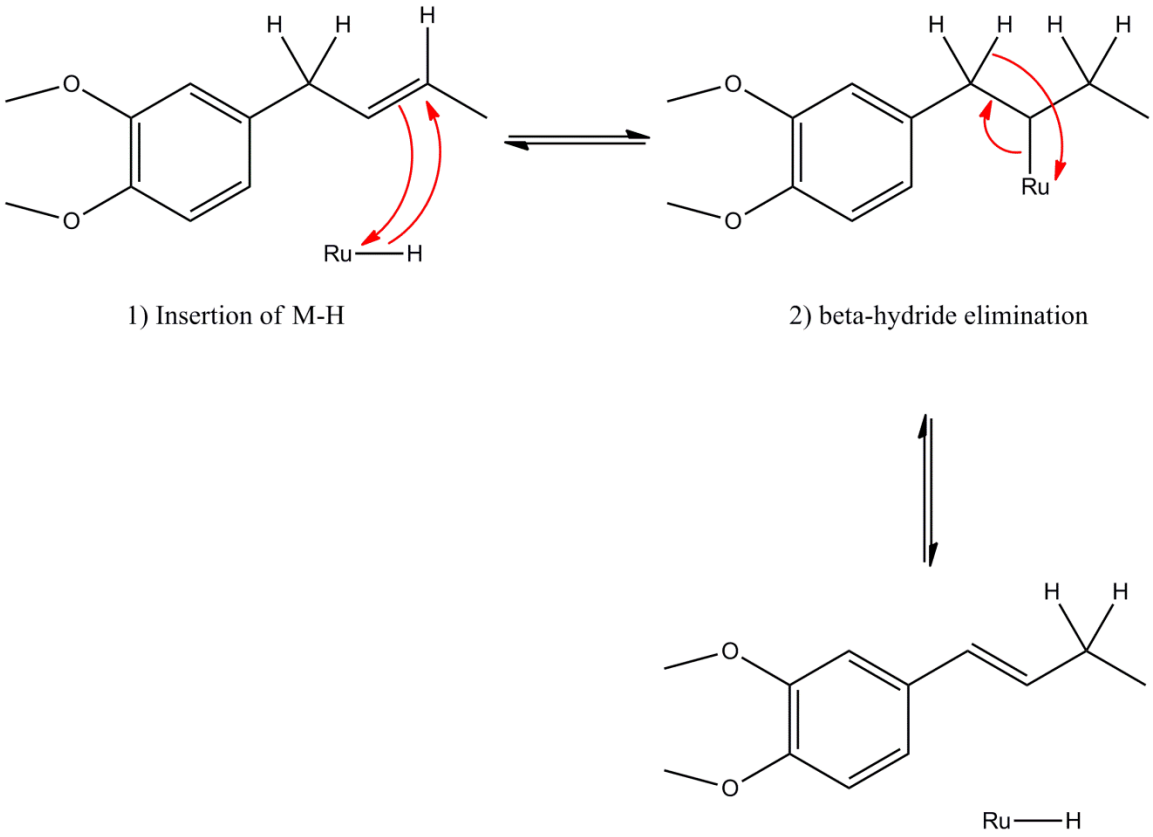

Figure 4: General Mechanism of Olefin Isomerization

Substrates

Two phenylpropenoid compounds, eugenol and 4-allyl-1,2-dimethoxybenzene, also known as methyl eugenol, were chosen as substrates in this research project. According to the aforementioned olefin classification scheme detailed in Table 1, both substrates are categorized as type 1 terminal olefins indicating that they demonstrate high reactivity in olefin cross metathesis and have a tendency to favor rapid

homodimerization, making them outstanding starting materials for the proposed tandem metathesis and isomerization sequence.[6]

Eugenol and methyl eugenol are natural components of many plant essential oils including cinnamon, cloves, and related spices.[15] Phenylpropenoid compounds are commonly used as substrates in olefin cross metathesis reactions as they are considered to be inexpensive precursors for more desirable and complex olefins.[14] Additionally, the relatively polar hydroxyl and methoxy functional groups present in eugenol and methyl eugenol conveniently facilitate the separation of dimerized and isomerized starting material from the nonpolar components of the crude reaction mixture during chromatographic purification. The structures of eugenol and methyl eugenol are shown below in Figures 5 and 6, respectively.

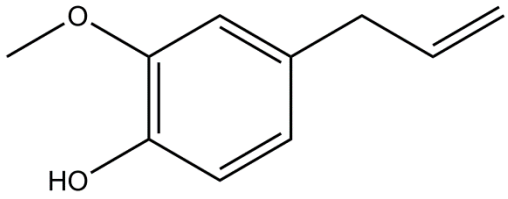

Figure 5: Structure of Eugenol

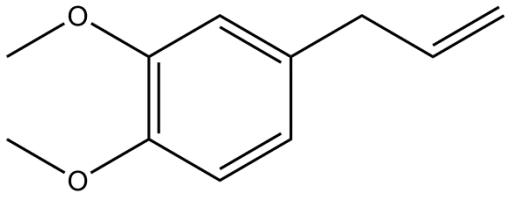

Figure 6: Structure of Methyl Eugenol

X-ray Crystallography

X-ray crystallography is an invaluable technique for determining the structures of crystalline organic, organometallic, and inorganic compounds. In X-ray crystallography, samples of crystalline compounds are exposed to X-rays which interact with the electrons of the analyte, resulting in unique diffraction patterns depending on the number and location of electrons in the atom or ion.[16] Diffraction of incident X-rays occurs because the range of wavelengths in the X-ray region of the electromagnetic spectrum is approximately equal to the distance between the planes of a crystal.[16, 17] X-ray diffraction methods are typically non-destructive and provide useful information regarding bond length, bond angles, and the relative locations of atoms and ions in a unit cell, or the smallest group of atoms of a substance that demonstrates the exact symmetry of the substance as a whole.[16]

The two primary categories of X-ray crystallography are powder X-ray diffraction and single-crystal X-ray diffraction. In powder X-ray diffraction, a polycrystalline sample composed of a multitude of small crystals oriented at random is irradiated with an X-ray beam causing the beam to be scattered in all directions resulting in an X-ray diffraction pattern.[16] Powder X-ray diffraction is useful for phase identification and obtaining general crystallographic information; however, it is unable to provide reliable three-dimensional structural information. On the other hand, single-crystal X-ray diffraction is a useful method to obtain structural information for compounds that form homogenous crystals with large surface areas.[16] In single-crystal X-ray diffraction, a diffractometer is used to rotate a single crystal of the compound of interest in three directions in an X-ray

beam in order to generate a diffraction pattern which is ultimately used to obtain three-dimensional structural information about the compound.[16-18]

In this research project, single-crystal X-ray diffraction was utilized to obtain structural data for the methyl eugenol dimer and the methyl eugenol isomerized dimer. Crystal data were obtained using a Bruker SMART X2S Single Crystal X-ray Diffractometer. The computer software SHELXS97 and SHELXL97 were used for guided crystal structure analysis and OLEX2 version 1.2 was used as the graphical user interface (GUI).

Chromatographic Methods

Chromatography includes a wide range of analytical techniques utilized by chemists in order to separate components of a mixture based on properties such as polarity, solubility, size, and ionic state.[19] Generally, the effectiveness of chromatographic methods is attributed to the movement of a mobile phase through a stationary phase. In the course of a separation, the stationary phase remains constant while the mobile phase is strategically adjusted to account for optimal elution of the desired product.[19, 20] The two chromatographic methods utilized in this research project were thin layer chromatography (TLC) and flash column chromatography.

Thin layer chromatography was used to assess the progress of product formation in the majority of the reactions conducted in this research project. TLC plates coated with silica gel were utilized as the polar stationary phase while various organic solvents were utilized as the nonpolar mobile phase.[21] Appropriate mobile phases were determined using trial and error. Screw cap jars were used as TLC developing chambers and were

filled with approximately 1 cm of nonpolar solvent. The spotted TLC plates were placed in the sealed chamber and capillary action drew up solvent to the indicated level of the TLC plate. Upon analysis of the developed TLC plate with short wave ultraviolet light, the presence of spots with different relative movements than the starting material indicated the formation of compounds with different polarities.[21]

Flash column chromatography was used to separate products of interest from undesired components in the crude reaction mixture such as unreacted starting material, side products, residual paraffin wax, and catalyst.[19] A large glass chromatography column with a stopcock and 500 mL solvent bulb was packed with a silica gel and n-hexanes slurry which served as the polar stationary phase. A series of organic solvent mixtures were prepared in a gradient of increasing polarity to serve as the nonpolar mobile phases. To continue, a glass adapter was clamped to the top of the chromatography column and a rubber hose was connected from the nitrogen output on the fume hood to an attachment on the glass adapter. A low pressure flow of inert nitrogen gas ensured more efficient separations in terms of lower time consumption and higher relative purity of the eluted fractions.[20]

In order to remove residual paraffin wax from small volumes of crude reaction mixture, micro-columns were prepared using Pasteur pipettes. Disposable Pasteur pipettes were packed with glass wool and silica gel and flushed with n-hexanes. After loading the aliquot onto the column, two mobile phases – nonpolar n-hexanes and relatively polar ethyl acetate were used to separate undesired components from products of interest.

Results and Discussion

The primary objective of this research project was to develop and optimize a synthetic procedure involving a one-pot, tandem olefin metathesis and isomerization sequence in order to synthesize resonance stabilized olefin compounds. In order to assess the feasibility of each individual reaction in the tandem sequence, both the dimerization and isomerization reactions were run independently under various reaction conditions. After this preliminary work, the tandem metathesis-isomerization sequence was run under various reaction conditions. Initially, eugenol was selected as the substrate of choice; however, after experiencing consistent challenges with the isomerization reaction using eugenol, it was abandoned and replaced with methyl eugenol, which provided better results. The following sections will further detail the individual dimerization, isomerization, and tandem reactions that were performed during the span of the research project.

Olefin Dimerization Reactions

Eugenol (compound **1**) was dimerized via an olefin cross metathesis reaction using the Grubbs second generation catalyst to yield compound **2**, (E)-4,4'-(2-butene-1,4-diyl)bis(2-methoxyphenol), shown in Figure 7. The reaction follows the general mechanism for olefin cross metathesis shown in Figure 2 when both starting olefins are the same compound. A mechanism for eugenol dimerization is shown in Figure 8 on the following page. In Figure 8, X indicates all of the unrepresented substituents of the Grubbs second generation catalyst, and Ph indicates the phenyl group attached to the carbene. This reaction was previously conducted by a former student in the Knight

research group and an identical procedure was followed. The reaction was performed on a large scale (grams) under static nitrogen. Reaction conditions were altered in order to assess the optimum environment to drive the reaction in the forward direction; however, reflux conditions were most frequently employed. Due to the large scale of the reaction, a significant amount of paraffin wax was present in the crude reaction mixture and both TLC and flash column chromatography were used to isolate the desired product which was an opaque crystalline solid.

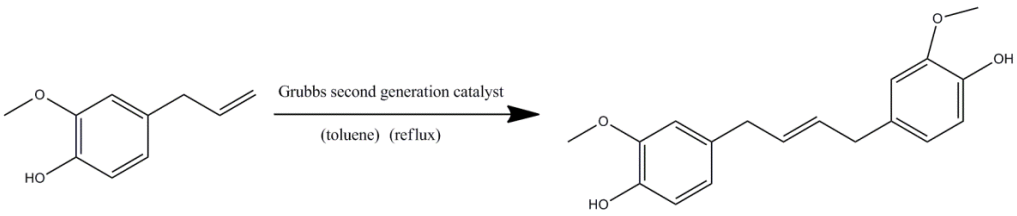

Figure 7: Dimerization of Eugenol

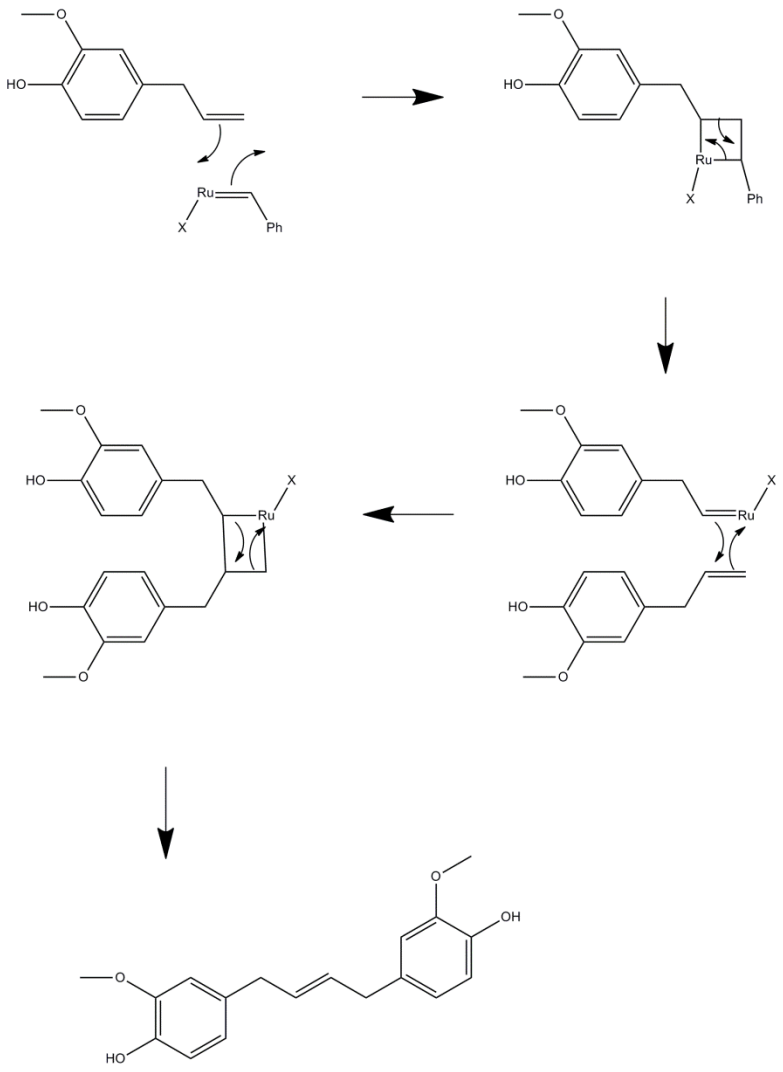

Figure 8: Eugenol Dimerization Mechanism

Similarly, methyl eugenol (compound **3**) was dimerized via an olefin cross metathesis reaction using the Grubbs second generation catalyst to yield compound **4**, (2*E*)-1,1'-(2-butene-1,4-diyl)bis(3,4-dimethoxybenzene), shown below in Figure 9. Again, the reaction follows the same general mechanism for olefin metathesis shown in Figure 2 when both starting olefins are the same compound. A mechanism for methyl eugenol dimerization is shown in Figure 10. In Figure 10, X indicates all of the unrepresented substituents of the Grubbs second generation catalyst, and Ph indicates the

phenyl group attached to the carbene. Generally, the dimerization reactions conducted with methyl eugenol as the substrate were run on a relatively small scale in order to conserve starting material. This, however, led to issues with product yield and further analysis of the product as much of the dimerized product continued to isomerize via degradation of the carbene catalyst. Furthermore, the remaining dimerized substrate was significantly affected by loss due to mass transfer. Aside from the scale, similar reaction conditions and purification techniques were employed for the dimerization of methyl eugenol as were previously employed for the dimerization of eugenol.

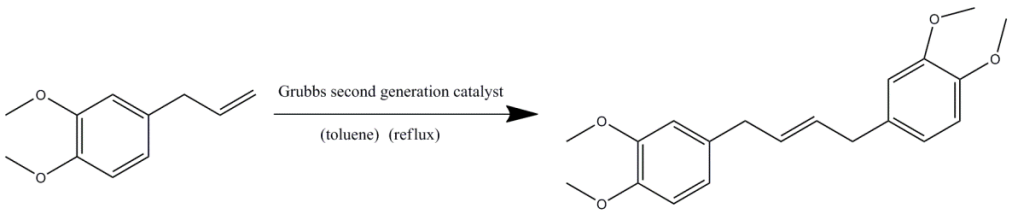

Figure 9: Methyl Eugenol Dimerization

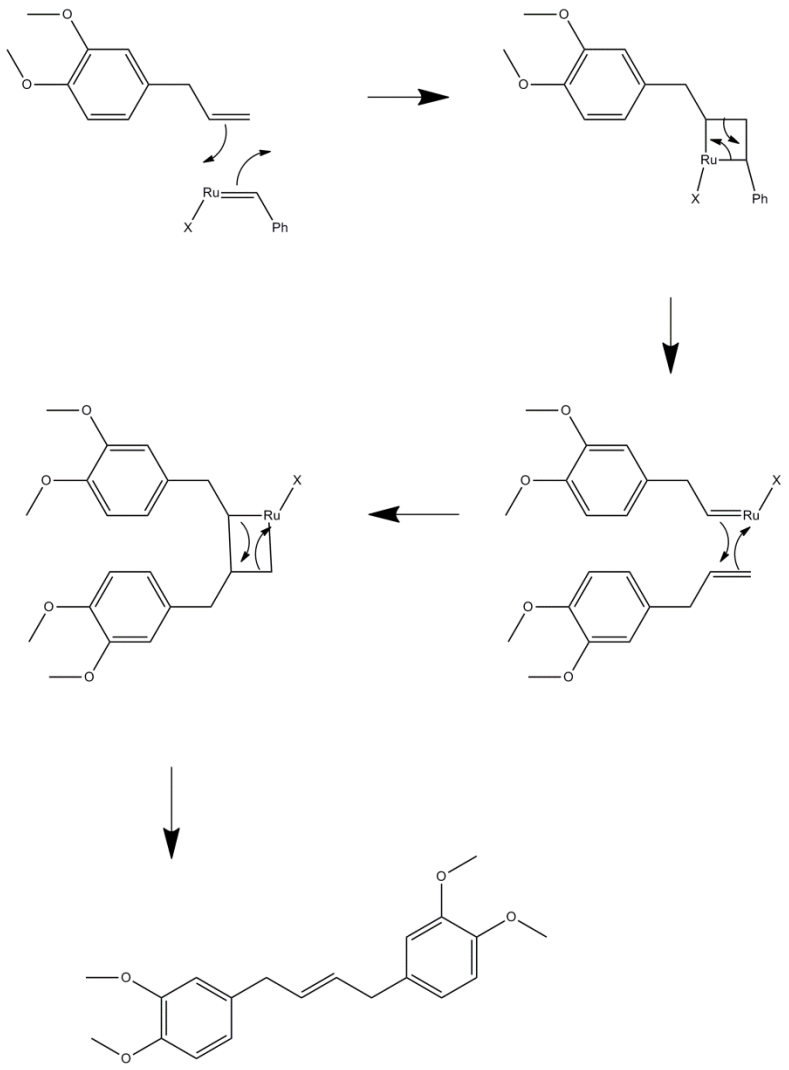

Figure 10: Methyl Eugenol Dimerization Mechanism

Table 2, on the following page, summarizes the reaction conditions and product ratios of all of the dimerization reactions conducted in this research project. Included above Table 2 is a key of all potential metathesis and isomerization products formed during the reaction. This key may be used with all subsequent tables.

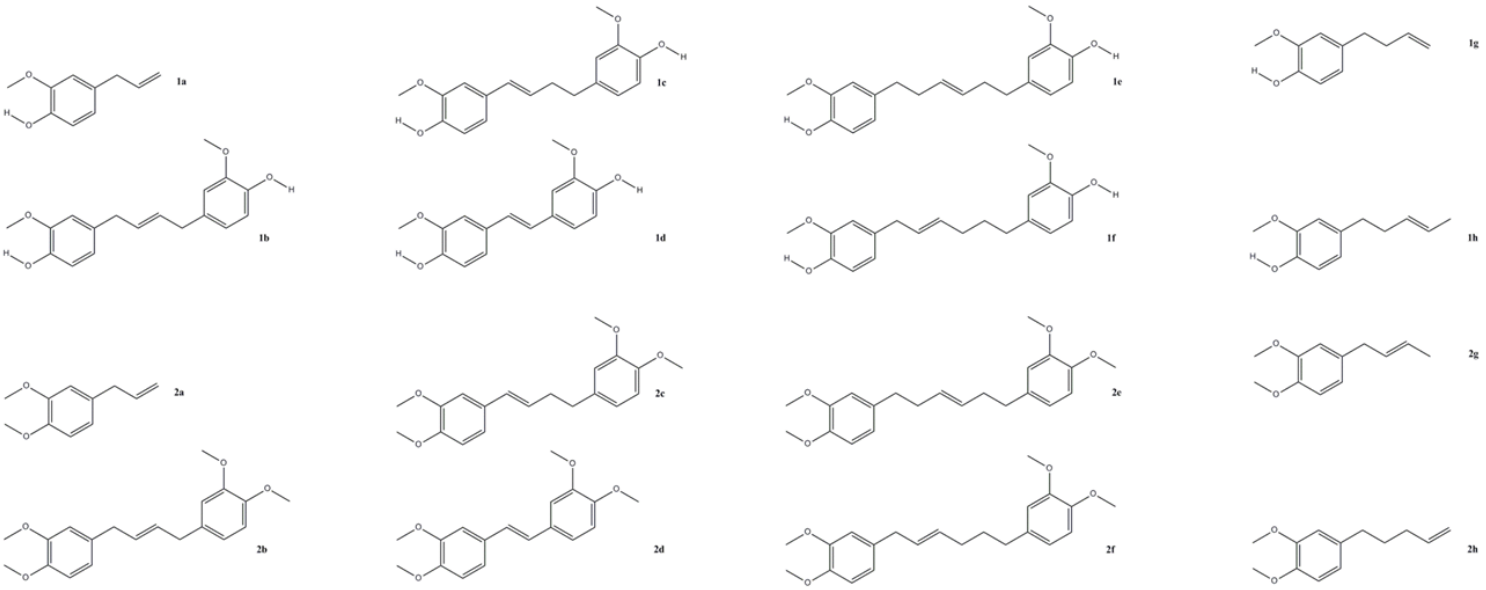

Table 2: Summary of Olefin Dimerization Reactions

Experiment	Substrate	Mol % Catalyst	Solvent	Temperature (°C)	Time	Hydride Source	Mol % Hydride	Product Ratio	Isolated Yield
AM1-1	1	1	n-Hexane	68	18 h	-----	-----	1a 89% 1b 11%	-----
AM9-1	2	1	n-Hexane	68	18 h	-----	-----	2d	-----
AM11-1	2	1	Pentane	36	18 h	-----	-----	2b 80% 2c 20%	-----
AM18-1	2	1	Toluene	111	25 h	-----	-----	2g 9% 2c 53% 2d 38%	2g 1.5% 2c 9% 2d 6.5%

Olefin Isomerization Reactions

Isolated olefin isomerization reactions were performed using eugenol and methyl eugenol in order to determine the effectiveness of the addition of an inorganic hydride

source at the start of the reaction in driving the reaction towards the formation of isomerized dimers of each of the respective starting materials. Eugenol was initially dimerized via the Grubbs second generation catalyst as described in the previous section. Theoretically, this dimerization should be followed by a rapid isomerization due to an excess of inorganic hydride resulting in the formation of resonance stabilized isomerized eugenol dimer; however, the combination of small reaction scale and undesired side reactions between the hydroxyl groups in eugenol and excess hydrogen in the reaction flask resulted in no detection of isomerized eugenol dimer via ^{1}H NMR after purification of the crude reaction mixtures.[22-24] Ultimately, eugenol was removed from consideration as a potential substrate for the isomerization and tandem metathesis-isomerization sequences.

Methyl eugenol (compound **3**) was initially dimerized to yield compound **4**. Due to an excess of inorganic hydride in the reaction flask, compound **4** was readily isomerized to compound **5**, 1,1'-(1-butene-1,4-diyl)bis(3,4-dimethoxybenzene), shown below in Figure 11. The isomerization reaction follows the general mechanism for olefin isomerization via insertion and β-hydride elimination shown in Figure 4. A mechanism for the isomerization of the methyl eugenol dimer is shown in Figure 12 on the following page. A variety of reaction conditions were utilized in order to determine the optimum conditions for conversion of methyl eugenol dimer to isomerized methyl eugenol dimer. Identical purification and analytical techniques were employed during the work up of the crude reaction mixture as the dimerization reactions.

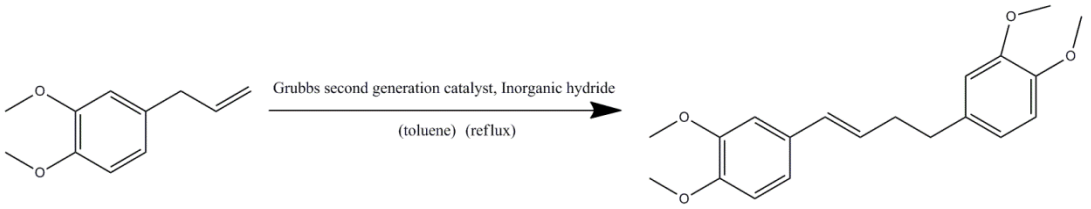

Figure 11: Methyl Eugenol Isomerization

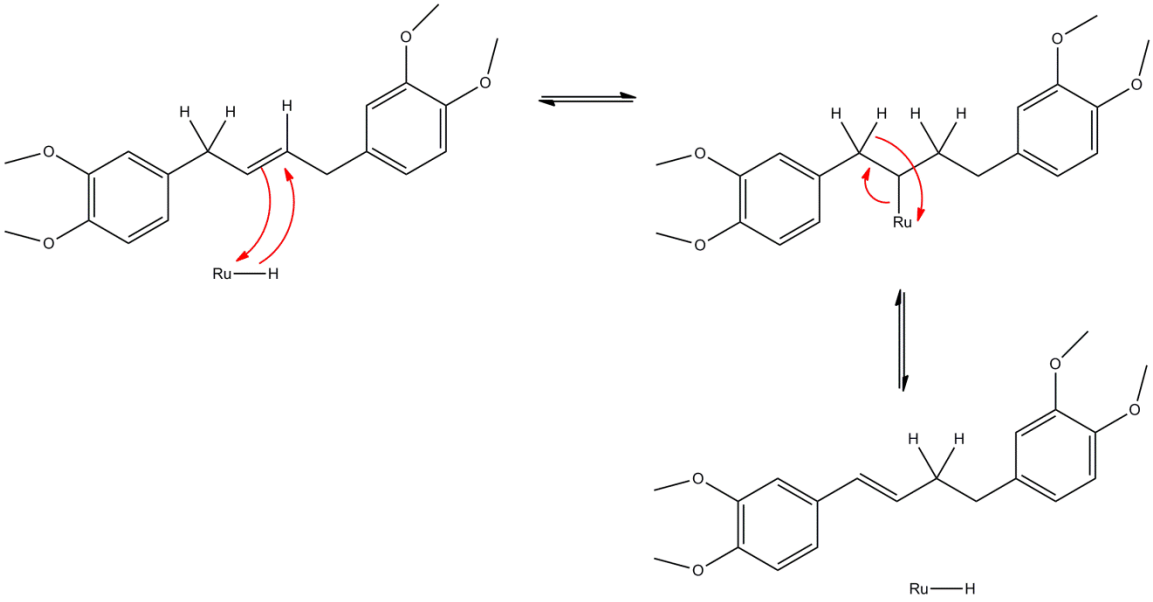

Figure 12: Methyl Eugenol Dimer Isomerization Mechanism

Table 3, shown on the following page, summarizes the reaction conditions and product ratios for all of the isomerization reactions conducted in this research project. An X-ray crystallographic structure of the isomerized methyl eugenol dimer was obtained from a small sample of crystalline material from Experiment AM13-1. This structure was obtained through X-ray diffraction analysis of crystals obtained through slow evaporation of the purified product in $CDCl_3$. The R-value of the structure is 4.74%, and a thermal ellipsoid plot of the crystal structure is shown in Figure 13 on the following page.

Table 3: Summary of Olefin Isomerization Reactions

Substrate	Mol % Catalyst	Solvent	Temperature (°C)	Time	Hydride Source	Mol % Hydride	Product Ratio	Isolated Yield
1	0.33	n-Hexane	20	65 h	$NaBH_4$	66	1a	-----
1	1	n-Hexane	20	65 h	$NaBH_4$	9	1a	-----
1	1	n-Hexane	68	5 h	$NaBH_4$	9	1h	-----
1	0.33	n-Hexane	68	17 h	$NaBH_4$	66	1h	-----
1	0.33	n-Hexane	68	24 h	NaH	66	1a	-----
2	0.33	n-Hexane	68	24 h	NaH	66	2c	-----
2	0.33	Pentane	36	23 h	NaH	66	2b	-----
2	0.33	Pentane	20	64 h	NaH	66	2b 80% 2c 20%	-----
2	0.33	Toluene	111	28 h	NaH	66	2b 18% 2c 82%	-----
2	0.33	Toluene	111	15 h	$NaBH_4$	66	2c	-----
2	0.33	Toluene	111	16 h	$NaBH_4$	66	2c 66% 2d 33% 2h 1%	2c 14.3% 2d 7.1% 2h 0.2%

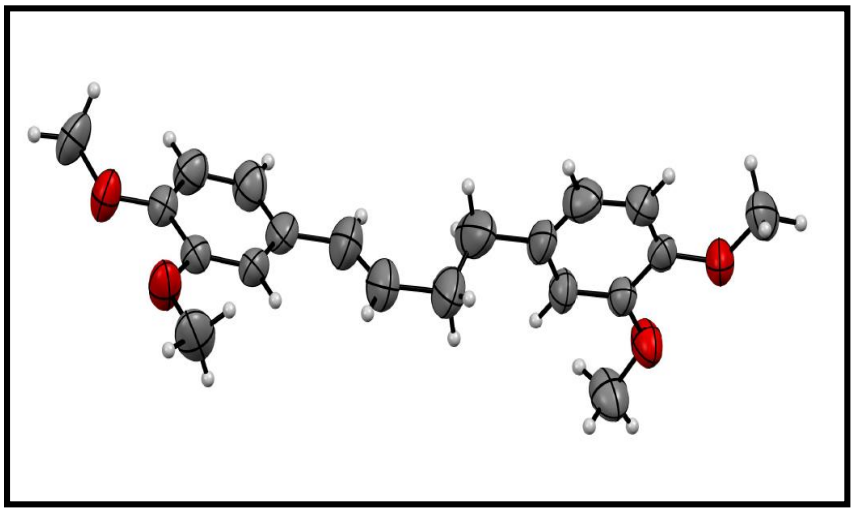

Figure 13: 1,1'-(1-butene-1,4-diyl)bis(3,4-dimethoxybenzene) Crystal Structure

Table 4: Acquisition and Crystal Data for 1,1'-(1-butene-1,4-diyl)bis(3,4-dimethoxybenzene)	
Formula	$C_{20}H_{24}O_4$
Molecular weight	324.00 g/mol
Crystal density	1.118 g/cm^3
Z	2
Acquisition temperature	199 K
Volume	898.0(2) Å^3
Space group	P -1
R	0.0474 (1147)
wR^2	0.1247 (1499)

Table 5: 1,1'-(1-butene-1,4-diyl)bis(3,4-dimethoxybenzene) Unit Cell Parameters		
a = 6.0878(8) Å	b = 10.0033(13) Å	c = 15.2626(19) Å
α = 99.832(4)°	β = 101.032(4)°	γ = 90.550(4)°

Tables 4 and 5, shown above, contain the acquisition and crystal data for the methyl eugenol isomerized dimer as well as the unit cell parameters for the methyl eugenol isomerized dimer, respectively.

Tandem Olefin Metathesis-Isomerization Reactions

As a general statement, only methyl eugenol (compound **3**) was utilized as a substrate in the tandem olefin metathesis-isomerization reactions due to previous unsuccessful attempts to isomerize the eugenol dimer. In the tandem sequence, compound **3** was ultimately isomerized to compound **5** as shown in Figure 14 on the following page. The general procedure for the tandem sequence began with a dimerization reaction in reflux conditions under static nitrogen. After reflux for a variable time, the crude reaction flask was allowed to cool and inorganic hydride was transferred to the reaction flask under active nitrogen. Upon hydride addition, the reaction was allowed to reflux under static nitrogen for a variable time. The crude reaction mixture

was purified and analyzed using identical techniques as the previous dimerization and isomerization reactions. The most significant challenge during the tandem sequence was the exposure of the reaction mixture to air during the addition of the inorganic hydride when such an effort had been made to maintain an air free environment using the schlenk line.[27] This problem was addressed through the use of a solid addition funnel which was loaded with an appropriate mass of inorganic hydride prior to the assembly of the reaction apparatus. A three-necked flask was used in place of a schlenk flask and the solid addition funnel was connected in such a way that minimal traces of hydride fell into solution during the dimerization portion of the tandem sequence. After post-dimerization cooling of the flask, applying tapping pressure on the solid addition funnel caused the hydride to fall into the solution without need of exposing the system to air. Table 4, shown on the following page, summarizes the reaction conditions and product ratios for all of the tandem olefin metathesis-isomerization reactions conducted in this research project.

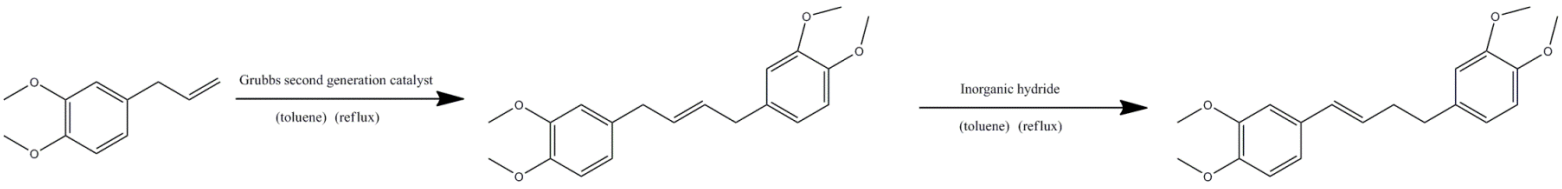

Figure 14: Methyl Eugenol Tandem Olefin Metathesis-Isomerization Mechanism

Table 6: Summary of Tandem Olefin Metathesis-Isomerization Reactions

Experiment	Substrate	Mol % Catalyst	Solvent	Temperature (°C)	Time	Hydride Source	Mol % Hydride	Product Ratio	Isolated Yield
AM10-1	1	0.33	n-Hexane	68	1) 11 h 2) 23 h	NaH	66	2d	-----
AM14-1	2	0.33	Pentane	36	64 h	NaH	66	2b 82% 2c 18%	-----
AM15-1	2	0.33	n-Hexane	1) 68 2) 23 3) 68	1) 23 h 2) 23 h 3) 19 h	NaH	66	2b 14% 2c 8% 2d 44% 2g 34%	-----

An X-ray crystallographic structure of the methyl eugenol dimer was obtained from a small sample of crystalline material from Experiment AM14-1. This structure was obtained through X-ray diffraction analysis of crystals obtained through slow evaporation of the purified product in $CDCl_3$.

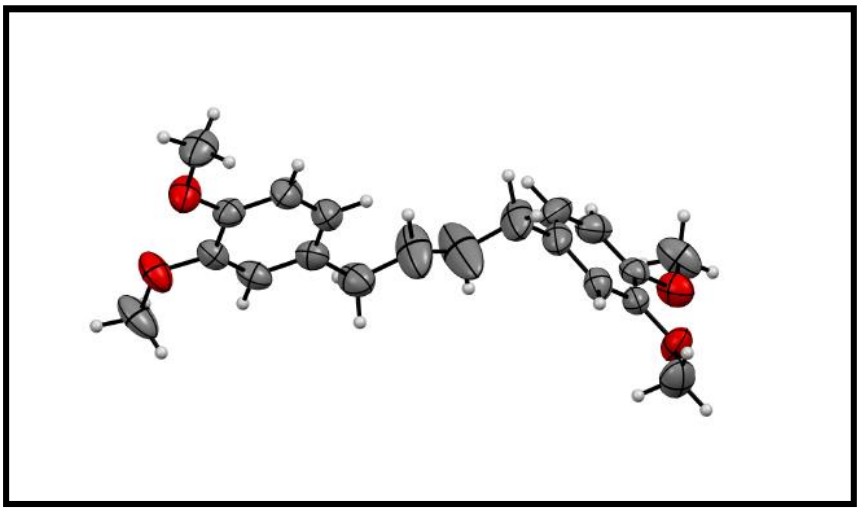

Figure 15: (2E)-1,1'-(2-butene-1,4-diyl)bis(3,4-dimethoxybenzene) Crystal Structure

Table 7: Acquisition and Crystal Data for (2E)-1,1'-(2-butene-1,4-diyl)bis(3,4-dimethoxybenzene)	
Formula	$C_{20}H_{20}O$
Molecular weight	296.00 g/mol
Crystal density	1.023 g/cm^3
Z	2
Acquisition temperature	199 K
Volume	897.0(3) Å^3
Space group	P -1
R	7.18%
wR^2	21.96%

Table 8: (2E)-1,1'-(2-butene-1,4-diyl)bis(3,4-dimethoxybenzene) Unit Cell Parameters		
a = 5.8616(9) Å	b = 10.0948(17) Å	c = 15.807(3) Å
α = 73.688(5)°	β = 88.554(5)°	γ = 90.550(4)°

A thermal ellipsoid plot of the methyl eugenol dimer crystal structure was show in Figure 15 on the previous page. Tables 7 and 8, shown above, contain the acquisition and crystal data for the methyl eugenol dimer as well as the unit cell parameters for the methyl eugenol dimer, respectively.

Experimental

General Comments

All solvents were used as obtained from the respective manufacturer and were not modified in any way. The mass ratio of the Grubbs second generation catalyst wax dispersion for experiments AM1-AM17 was 10 g paraffin wax per 1 gram catalyst while the mass ratio of the Grubbs second generation catalyst wax dispersion for Experiments AM18-AM19 was 10 g paraffin wax per 1.1 gram catalyst. A JEOL 400 MHz FT-NMR was used to perform all ^{1}H NMR and ^{13}C NMR experiments and NMR data were analyzed using JEOL Delta NMR software version 4.3.6. All crystal samples were

mounted on a Bruker SPINE-Pin using Krytox vacuum grease. A Bruker SMART X2S Single Crystal X-ray Diffractometer was used to analyze all crystal samples and obtain structural data. Structural solutions were solved using SHELXS97 and SHELXL97 through the OLEX2 version 1.2 GUI. Lastly, due to the generally unpredictable nature of olefin cross metathesis reactions, poor product yields were often the norm for the experiments performed in this research project. In the following sections, representative procedures are provided in detail for the proposed syntheses of the methyl eugenol dimer and the methyl eugenol isomerized dimer, respectively.

Methyl eugenol dimer

Methyl eugenol (8.000 g) and 11% Grubbs second generation catalyst wax dispersion (3.460 g) in a 100:1 equivalence ratio underwent reflux in 125 mL of toluene under static nitrogen for 25 hours. The crude reaction mixture was purified into distinct components via flash column chromatography with a silica gel stationary phase. A solvent gradient of varying concentrations of n-hexane, tert-butyl methyl ether, ethyl acetate, and methanol were used to separate mixture components based on polarity. Thirty-two fractions were collected from the chromatography column and were left out for slow evaporation in the fume hood. Crystal formation occurred immediately after elution for several of the fractions. Fractions with substantial crystal formation had a deep amber color. TLC was performed on the fractions using tert-butyl methyl ether as the developing solvent. Crystals were manually transferred to vials and characterized via ^{1}H NMR spectroscopy using $CDCl_3$ as the solvent. Upon analysis of the ^{1}H NMR spectra, it was determined that none of the isolated crystals were methyl eugenol dimer. Instead, the

majority products were the methyl eugenol isomerized dimer and undesired products formed as a result of continued cross metathesis and isomerization activity of the carbene catalyst. ^{1}H NMR (400 MHz, CDCl3, ppm):

Methyl eugenol isomerized dimer

Methyl eugenol (8.000 g), 11% Grubbs second generation catalyst wax dispersion (3.460 g) in a 100:1 equivalence ratio, and 2.169 g of $NaBH_4$ underwent reflux in 125 mL of toluene under static nitrogen for 16 hours. The crude reaction mixture was purified into distinct components via flash column chromatography with a silica gel stationary phase. A solvent gradient of varying concentrations of n-hexane, tert-butyl methyl ether, and ethyl acetate were used to separate mixture components based on polarity. Twenty-four fractions were collected from the chromatography column and were left out for slow evaporation in the fume hood. Crystal formation occurred immediately after elution for several of the fractions. Fractions with substantial crystal formation had a deep amber color. Crystals were manually transferred to vials and characterized via ^{1}H NMR spectroscopy using $CDCl_3$ as the solvent. The crystals of the methyl eugenol isomerized dimer were isolated with a yield of 1.144 g (14.30%) and a product ratio of 66%. Other crystals included undesired cross metathesis and isomerization side products.

Future Works

The results of this project have provided a foundation for future work in optimizing the conditions for a tandem olefin metathesis-isomerization sequence in order to synthesize conjugated aromatic olefins. Several obstacles remain in the development of

this synthetic procedure, with the greatest being the adjustment of reaction conditions to maximize product yield. Future work in utilizing the one-pot, tandem olefin metathesis-isomerization sequence for the synthesis of analogs to natural plant derivatives continues to be the ultimate goal of this research project.

Conclusion

The primary objective of this research project was to assess the feasibility of a one-pot tandem olefin metathesis-isomerization sequence in order to synthesize resonance stabilized olefins using terminal aromatic olefin substrates and the Grubbs second generation catalyst. Overall, the tandem sequence was successful in the preparation of isomerized dimers from the respective starting olefin; however, the remaining challenge is increasing product yield and selectivity towards the isomerized dimer of the starting material. Additionally, crystal structures were obtained for the methyl eugenol dimer and the methyl eugenol isomerized dimer which added further credence to the feasibility of the individual reactions in the tandem sequence as well as the proposed tandem metathesis-isomerization sequence itself.

Acknowledgments

Funding for this research project was generously provided by the National Science Foundation, The University of Tennessee at Chattanooga Department of Chemistry Grote Fund, and The University of Tennessee at Chattanooga Provost Student Research Award. Furthermore, a 5 gram sample of the Grubbs second generation catalyst was graciously donated to Dr. Knight's research group by Materia, Inc.

References

1. Hong, J., Natural product synthesis at the interface of chemistry and biology. Chemistry (Weinheim an der Bergstrasse, Germany) 2014, 20 (33), 10204-10212.
2. Mol, J. C., Industrial applications of olefin metathesis. Journal of Molecular Catalysis A: Chemical 2004, 213 (1), 39-45.
3. Bruice, P. Organic Chemistry, 7th ed.; Pearson Education: New Jersey, 2014; pp 548-550.
4. Grubbs, R. H., Olefin metathesis. Tetrahedron 2004, 60 (34), 7117-7140.
5. Taber, D. F.; Frankowski, K. J., Grubbs's Cross Metathesis of Eugenol with cis-2-Butene-1,4-diol To Make a Natural Product. An Organometallic Experiment for the Undergraduate Lab. Journal of Chemical Education 2006, 83 (2), 283.
6. Chatterjee, A. K.; Choi, T.-L.; Sanders, D. P.; Grubbs, R. H., A General Model for Selectivity in Olefin Cross Metathesis. Journal of the American Chemical Society 2003, 125 (37), 11360-11370.
7. Grubbs, R. H.; Carr, D. D.; Hoppin, C.; Burk, P. L., Consideration of the mechanism of the metal catalyzed olefin metathesis reaction. Journal of the American Chemical Society 1976, 98 (12), 3478-3483.
8. Schrock, R. R.; Hoveyda, A. H., Molybdenum and Tungsten Imido Alkylidene Complexes as Efficient Olefin-Metathesis Catalysts. Angewandte Chemie International Edition 2003, 42 (38), 4592-4633.
9. Hoveyda, A. H.; Zhugralin, A. R., The remarkable metal-catalysed olefin metathesis reaction. Nature 2007, 450 (7167), 243-251.
10. Scholl, M.; Ding, S.; Lee, C. W.; Grubbs, R. H., Synthesis and Activity of a New Generation of Ruthenium-Based Olefin Metathesis Catalysts Coordinated with 1,3-Dimesityl-4,5-dihydroimidazol-2-ylidene Ligands. Organic Letters 1999, 1 (6), 953-956.
11. Formentín, P.; Gimeno, N.; Steinke, J. H. G.; Vilar, R., Reactivity of Grubbs' Catalysts with Urea- and Amide-Substituted Olefins. Metathesis and Isomerization. The Journal of Organic Chemistry 2005, 70 (20), 8235-8238.
12. Schmidt, B., Catalysis at the Interface of Ruthenium Carbene and Ruthenium Hydride Chemistry: Organometallic Aspects and Applications to Organic Synthesis. European Journal of Organic Chemistry 2004, 2004 (9), 1865-1880.
13. Taber, D. F.; Frankowski, K. J., Grubbs' Catalyst in Paraffin: An Air-Stable Preparation for Alkene Metathesis. The Journal of Organic Chemistry 2003, 68 (15), 6047-6048.
14. Hassam, M.; Taher, A.; Arnott, G. E.; Green, I. R.; van Otterlo, W. A. L., Isomerization of Allylbenzenes. Chemical Reviews 2015, 115 (11), 5462-5569.
15. Mallavarapu, G. R.; Ramesh, S.; Chandrasekhara, R. S.; Rajeswara Rao, B. R.; Kaul, P. N.; Bhattacharya, A. K., Investigation of the essential oil of cinnamon leaf grown at Bangalore and Hyderabad. Flavour and Fragrance Journal 1995, 10 (4), 239-242.
16. Weller, M.; Overton, T.; Rourke, J.; Armstrong, F. Inorganic Chemistry, 6th ed.; Oxford University Press: Oxford, 2014; pp 234-238.
17. Atkins, P.; de Paula, J.; Atkins' Physical Chemistry, 10th ed.; Oxford University Press: New Delhi, 2014; pp 742-748.

18. Lapidus, S. H.; Stephens, P. W.; Arora, K. K.; Shattock, T. R.; Zaworotko, M. J., A Comparison of Cocrystal Structure Solutions from Powder and Single Crystal Techniques. Crystal Growth & Design 2010, 10 (10), 4630-4637.
19. Skoog, D.A; Holler, F. J.; Crouch, S. R. Principles of Instrumental Analysis, 6th ed.; Thompson Corporation: Belmont, California, 2007; pp 829-841.
20. Novak, J.; Janak, J., Liquid Column Chromatography: A Survey of Modern Techniques and Applications. Elsevier Scientific Publishing Company: Amsterdam, 1975.
21. Harris, D.C. Exploring Chemical Analysis; Jeremy P. W.H. Freeman and Company: New York, 2013; pp 510-528.
22. Schmidt, B., Ruthenium-Catalyzed Olefin Metathesis Double-Bond Isomerization Sequence. The Journal of Organic Chemistry 2004, 69 (22), 7672-7687.
23. Schmidt, B.; Pohler, M., Tandem olefin metathesis/hydrogenation at ambient temperature: activation of ruthenium carbene complexes by addition of hydrides. Organic & Biomolecular Chemistry 2003, 1 (14), 2512-2517.
24. Clark, J. R.; Griffiths, J. R.; Diver, S. T., Ruthenium Hydride-Promoted Dienyl Isomerization: Access to Highly Substituted 1,3-Dienes. Journal of the American Chemical Society 2013, 135 (9), 3327-3330.
25. Courchay, F. C.; Sworen, J. C.; Ghiviriga, I.; Abboud, K. A.; Wagener, K. B., Understanding Structural Isomerization during Ruthenium-Catalyzed Olefin Metathesis: A Deuterium Labeling Study. Organometallics 2006, 25 (26), 6074-6086.
26. de la Torre, M. C.; Deometrio, A. M.; Álvaro, E.; García, I.; Sierra, M. A., Synthesis of α-Onoceradiene-like Terpene Dimers by Intermolecular Metathesis Processes. Organic Letters 2006, 8 (4), 593-596.
27. Guidone, S.; Songis, O.; Nahra, F.; Cazin, C. S. J., Conducting Olefin Metathesis Reactions in Air: Breaking the Paradigm. ACS Catalysis 2015, 5 (5), 2697-2701.
28. Hong, S. H.; Sanders, D. P.; Lee, C. W.; Grubbs, R. H., Prevention of Undesirable Isomerization during Olefin Metathesis. Journal of the American Chemical Society 2005, 127 (49), 17160-17161.
29. Masuda, T.; Jitoe, A., Phenylbutenoid monomers from the rhizomes of Zingiber cassumunar. Phytochemistry 1995, 39 (2), 459-461.
30. Schmidt, B., An Olefin Metathesis/Double Bond Isomerization Sequence Catalyzed by an In Situ Generated Ruthenium Hydride Species. European Journal of Organic Chemistry 2003, 2003 (5), 816-819.
31. Scholte, A. A.; An, M. H.; Snapper, M. L., Ruthenium-Catalyzed Tandem Olefin Metathesis−Oxidations. Organic Letters 2006, 8 (21), 4759-4762.

Appendix I

(2E)-1,1'-(2-butene-1,4-diyl)bis(3,4-dimethoxybenzene) Report

Table 1. Crystal data and structure refinement for am11dimethyleugenoldimer.

Identification code	am11dimethyleugenoldimer	
Empirical formula	C20 H20 O	
Formula weight	276.36	
Temperature	200(2) K	
Wavelength	0.71073 Å	
Crystal system	Triclinic	
Space group	P -1	
Unit cell dimensions	a = 5.8616(9) Å	α = 73.688(5)°
	b = 10.0948(17) Å	β = 88.554(5)°
	c = 15.807(3) Å	γ = 88.047(5)°
Volume	897.0(3) $Å^3$	
Z	2	
Density (calculated)	1.023 Mg/cm^3	
Absorption coefficient	0.061 mm^{-1}	
F(000)	296	
Crystal size	0.20 x 0.40 x 0.60 mm^3	
Theta range for data collection	1.34 to 24.27°	
Index ranges	-6<=h<=6, -11<=k<=11, -18<=l<=18	
Reflections collected	15841	
Independent reflections	2881 [R(int) = 0.0433]	
Completeness to theta = 24.27°	98.9%	
Absorption correction	Multiscan	
Max. and min. transmission	0.9878 and 0.9082	
Refinement method	Full-matrix least-squares on F^2	
Data / restraints / parameters	2881 / 0 / 221	
Goodness-of-fit on F^2	1.160	
Final R indices [I>2sigma(I)]	R1 = 0.0718, wR2 = 0.1964	
R indices (all data)	R1 = 0.1025, wR2 = 0.2196	
Largest diff. peak and hole	0.421 and -0.264	

Table 2. Atomic coordinates ($x10^4$) and equivalent isotropic displacement parameters ($Å^2x10^3$) for am11dimethyleugenoldimer.

U(eq) is defined as one third of the trace of the orthogonalized U^{ij} tensor.

	x	y	z	U(eq)
O1	11150(5)	5514(3)	877(2)	66(1)
O2	3492(4)	8769(3)	8458(2)	67(1)
O3	7713(5)	7223(3)	661(2)	62(1)
O4	6947(5)	10264(3)	7877(2)	71(1)
C1	12959(7)	4511(5)	958(4)	82(2)
C2	10081(6)	5620(3)	1632(2)	48(1)
C3	8168(6)	6535(3)	1516(2)	45(1)
C4	6932(6)	6673(4)	2233(2)	53(1)
C5	7525(8)	5938(5)	3085(3)	64(1)
C6	6096(10)	6079(6)	3869(3)	97(2)
C7	6853(16)	7164(9)	4242(5)	171(4)
C8	6966(11)	7517(8)	4816(4)	118(2)
C9	7749(8)	8556(5)	5223(3)	75(1)
C10	6541(7)	8577(4)	6083(3)	57(1)
C11	4667(7)	7818(4)	6400(3)	62(1)
C12	3582(7)	7852(4)	7181(3)	63(1)
C13	4384(6)	8668(4)	7672(2)	52(1)
C14	1636(7)	7889(5)	8829(3)	79(1)
C15	5900(9)	8238(5)	507(3)	82(1)
C16	9437(9)	5080(5)	3187(3)	74(1)
C17	10712(7)	4920(4)	2469(3)	64(1)
C18	6300(6)	9472(4)	7360(2)	50(1)
C19	8832(8)	11147(5)	7558(4)	88(2)
C20	7357(6)	9414(4)	6581(3)	55(1)

Table 3. Bond lengths (Å) and angles (°) for am11dimethyleugenoldimer.

O1-C2	1.364(4)
O1-C1	1.424(5)
O2-C13	1.365(4)
O2-C14	1.434(5)
O3-C3	1.363(4)
O3-C15	1.428(5)
O4-C18	1.362(4)
O4-C19	1.434(5)
C2-C17	1.366(5)
C2-C3	1.410(5)
C3-C4	1.367(5)
C4-C5	1.390(5)
C5-C16	1.378(6)
C5-C6	1.516(6)
C6-C7	1.467(8)
C7-C8	1.069(8)
C8-C9	1.467(7)
C9-C10	1.522(6)
C10-C11	1.364(5)
C10-C20	1.408(5)
C11-C12	1.382(6)
C12-C13	1.381(5)
C13-C18	1.405(5)
C16-C17	1.388(6)
C18-C20	1.379(5)
C2-O1-C1	117.6(3)
C13-O2-C14	116.8(3)
C3-O3-C15	117.3(3)
C18-O4-C19	116.5(3)
O1-C2-C17	125.5(4)
O1-C2-C3	115.6(3)
C17-C2-C3	118.9(4)
O3-C3-C4	125.2(3)
O3-C3-C2	114.9(3)
C4-C3-C2	120.0(3)

C3-C4-C5	121.5(4)
C16-C5-C4	117.6(4)
C16-C5-C6	121.7(4)
C4-C5-C6	120.7(4)
C7-C6-C5	113.6(4)
C8-C7-C6	146.7(7)
C7-C8-C9	148.6(7)
C8-C9-C10	115.3(4)
C11-C10-C20	117.6(4)
C11-C10-C9	122.8(4)
C20-C10-C9	119.6(4)
C10-C11-C12	122.2(4)
C13-C12-C11	120.4(4)
O2-C13-C12	125.9(3)
O2-C13-C18	115.2(3)
C12-C13-C18	118.9(3)
C5-C16-C17	121.8(4)
C2-C17-C16	120.1(4)
O4-C18-C20	125.5(3)
O4-C18-C13	115.0(3)
C20-C18-C13	119.5(3)
C18-C20-C10	121.5(4)

Table 4. Anisotropic displacement parameters ($Å^2x10^3$) for am11dimethyleugenoldimer.

The anisotropic displacement factor exponent takes the form:
$-2\pi^2[h^2 a^{*2} U^{11} + ... + 2 h k a^* b^* U^{12}]$

	U^{11}	U^{22}	U^{33}	U^{23}	U^{13}	U^{12}
O1	67(2)	60(2)	73(2)	-24(1)	-24(1)	5(1)
O2	55(2)	92(2)	57(2)	-23(2)	-23(2)	-27(2)
O3	79(2)	65(2)	42(2)	-16(1)	-16(1)	17(1)
O4	54(2)	77(2)	97(2)	-49(2)	-49(2)	-24(1)
C1	57(3)	69(3)	129(4)	-44(3)	-44(3)	0(2)
C2	51(2)	41(2)	53(2)	-11(2)	-11(2)	-11(2)
C3	50(2)	44(2)	42(2)	-15(2)	-15(2)	-6(2)
C4	51(2)	60(2)	54(2)	-24(2)	-24(2)	-11(2)
C5	74(3)	73(3)	46(2)	-17(2)	-17(2)	-32(2)
C6	118(4)	126(4)	60(3)	-42(3)	-42(3)	-61(4)
C7	242(9)	189(7)	124(5)	-107(6)	-107(6)	-145(7)
C8	112(5)	172(6)	101(4)	-87(5)	-87(5)	-63(4)
C9	88(3)	68(3)	73(3)	-25(2)	-25(2)	-21(2)
C10	60(2)	47(2)	60(2)	-11(2)	-11(2)	-1(2)
C11	72(3)	59(2)	55(2)	-17(2)	-17(2)	-14(2)
C12	59(3)	65(3)	62(3)	-11(2)	-11(2)	-21(2)
C13	47(2)	56(2)	49(2)	-9(2)	-9(2)	-9(2)

	U^{11}	U^{22}	U^{33}	U^{23}	U^{13}	U^{12}
C14	64(3)	102(4)	64(3)	-10(2)	-10(2)	-28(3)
C15	97(4)	74(3)	73(3)	-21(2)	-21(2)	30(3)
C16	88(3)	73(3)	48(2)	5(2)	5(2)	-23(3)
C17	59(3)	53(2)	73(3)	-4(2)	-4(2)	-9(2)
C18	46(2)	43(2)	63(2)	-17(2)	-17(2)	-3(2)
C19	64(3)	81(3)	139(5)	-63(3)	-63(3)	-33(2)
C20	50(2)	44(2)	71(3)	-15(2)	-15(2)	-6(2)

Table 5. Hydrogen coordinates ($x10^4$) and isotropic displacement parameters ($Å^2x10^3$) for am11dimethyleugenoldimer.

	x	y	z	U(eq)
H1A	14237	4768	1262	123
H1B	13465	4469	370	123
H1C	12420	3605	1298	123
H4	5637	7286	2146	64
H6	4830	5518	4098	117
H9	8928	9173	4967	90
H11	4088	7247	6074	74
H12	2277	7311	7380	75

	x	y	z	U(eq)
H14A	325	8134	8436	118
H14B	1207	8006	9407	118
H14C	2107	6924	8895	118
H15A	4447	7787	698	122
H15B	5845	8723	-124	122
H15C	6163	8903	840	122
H16	9895	4584	3764	88
H17	12026	4323	2559	77
H19A	10175	10588	7476	132
H19B	9172	11648	7986	132
H19C	8438	11809	6993	132
H20	8664	9950	6376	67

Appendix II

1,1'-(1-butene-1,4-diyl)bis(3,4-dimethoxybenzene) Report

Table 1. Crystal data and structure refinement for am_k_09182015.

Identification code	am_k_09182015	
Empirical formula	C18 H22 O4	
Formula weight	302.36	
Temperature	199(2) K	
Wavelength	0.71073 Å	
Crystal system	Triclinic	
Space group	P -1	
Unit cell dimensions	a = 6.0878(8) Å	α = 99.832(4)°
	b = 10.0033(13) Å	β = 101.032(4)°
	c = 15.2626(19) Å	γ = 90.550(4)°
Volume	898.0(2) $Å^3$	
Z	2	
Density (calculated)	1.118 Mg/cm^3	
Absorption coefficient	0.078 mm^{-1}	
F(000)	324	
Crystal size	0.10 x 0.30 x 0.40 mm^3	
Theta range for data collection	1.38 to 19.27°	
Index ranges	-5<=h<=5, -9<=k<=9, -14<=l<=14	
Reflections collected	9861	
Independent reflections	1510 [R(int) = 0.0412]	
Completeness to theta = 19.27°	100.0%	
Absorption correction	Multiscan	
Max. and min. transmission	0.9922 and 0.8569	
Refinement method	Full-matrix least-squares on F^2	
Data / restraints / parameters	1510 / 0 / 221	
Goodness-of-fit on F^2	1.104	
Final R indices [I>2sigma(I)]	R1 = 0.0529, wR2 = 0.1568	
R indices (all data)	R1 = 0.0727, wR2 = 0.1802	
Largest diff. peak and hole	0.243 and -0.186	

Table 2. Atomic coordinates ($x10^4$) and equivalent isotropic displacement parameters ($Å^2x10^3$) for am_k_09182015.

U(eq) is defined as one third of the trace of the orthogonalized U^{ij} tensor.

	x	y	z	U(eq)
O1	2627(5)	1556(4)	8448(2)	72(1)
O2	11561(6)	4282(4)	928(2)	76(1)
O3	8141(6)	2653(4)	665(2)	75(1)
O4	5820(6)	113(4)	8010(3)	76(1)
C1	1053(9)	2463(6)	8783(4)	87(2)
C2	3284(8)	1752(5)	7676(3)	52(1)
C3	2400(8)	2659(6)	7132(4)	70(2)
C4	3244(9)	2795(6)	6376(4)	74(2)
C5	4957(10)	2044(6)	6129(4)	70(2)
C6	5875(12)	2270(7)	5321(4)	95(2)
C7	7498(11)	1655(6)	5001(4)	92(2)
C8	8427(12)	1941(7)	4191(4)	102(2)
C9	8062(13)	3212(7)	3938(4)	115(2)
C10	9125(11)	3488(6)	3155(4)	70(2)
C11	11008(11)	4324(6)	3281(4)	78(2)
C12	11900(8)	4613(5)	2574(4)	66(2)
C13	10886(8)	4054(5)	1700(4)	53(1)
C14	13411(9)	5225(6)	1029(4)	87(2)
C15	8153(8)	2913(5)	2277(4)	60(1)
C16	8990(8)	3182(5)	1559(3)	53(1)
C17	6365(10)	1639(6)	480(4)	90(2)
C18	5840(8)	1127(5)	6678(4)	61(1)
C19	5035(8)	982(5)	7433(3)	55(1)
C20	7603(9)	-718(6)	7807(5)	98(2)

Table 3. Bond lengths (Å) and angles (°) for am_k_09182015.

O1-C2	1.358(5)
O1-C1	1.431(6)
O2-C13	1.373(6)
O2-C14	1.430(6)
O3-C16	1.373(5)
O3-C17	1.429(6)
O4-C19	1.366(5)
O4-C20	1.423(6)
C2-C3	1.377(7)
C2-C19	1.391(6)
C3-C4	1.377(7)
C4-C5	1.364(7)
C5-C18	1.390(7)
C5-C6	1.497(8)
C6-C7	1.299(8)
C7-C8	1.521(8)
C8-C9	1.399(8)
C9-C10	1.526(8)
C10-C15	1.379(7)
C10-C11	1.376(7)
C11-C12	1.368(7)
C12-C13	1.377(7)
C13-C16	1.400(6)
C15-C16	1.359(6)
C18-C19	1.365(6)
C2-O1-C1	117.6(4)
C13-O2-C14	117.8(4)
C16-O3-C17	117.3(4)
C19-O4-C20	117.8(4)
O1-C2-C3	125.6(5)
O1-C2-C19	116.3(5)
C3-C2-C19	118.0(5)
C4-C3-C2	120.5(5)
C5-C4-C3	122.1(5)

C4-C5-C18	117.2(5)
C4-C5-C6	120.0(6)
C18-C5-C6	122.7(6)
C7-C6-C5	127.8(7)
C6-C7-C8	126.3(6)
C9-C8-C7	117.6(6)
C8-C9-C10	116.0(6)
C15-C10-C11	117.6(5)
C15-C10-C9	119.6(6)
C11-C10-C9	122.7(6)
C12-C11-C10	122.4(5)
C11-C12-C13	119.3(5)
O2-C13-C12	125.5(5)
O2-C13-C16	115.4(5)
C12-C13-C16	119.1(5)
C16-C15-C10	121.4(5)
C15-C16-O3	125.4(5)
C15-C16-C13	120.1(5)
O3-C16-C13	114.5(4)
C19-C18-C5	121.5(5)
C18-C19-O4	125.1(5)
C18-C19-C2	120.6(5)
O4-C19-C2	114.2(4)

Table 4. Anisotropic displacement parameters ($Å^2x10^3$) for am_k_09182015.

The anisotropic displacement factor exponent takes the form:
$-2\pi^2[h^2 a^{*2} U^{11} + ... + 2 h k a^* b^* U^{12}]$

	U^{11}	U^{22}	U^{33}	U^{23}	U^{13}	U^{12}
O1	71(2)	94(3)	62(2)	24(2)	24(2)	27(2)
O2	87(3)	79(3)	70(3)	13(2)	13(2)	-10(2)
O3	87(3)	85(3)	53(3)	17(2)	17(2)	-23(2)
O4	76(2)	75(3)	94(3)	36(2)	36(2)	30(2)
C1	82(4)	102(5)	84(4)	7(4)	7(4)	22(4)
C2	53(3)	58(3)	46(3)	10(3)	10(3)	4(3)
C3	70(4)	73(4)	67(4)	9(3)	9(3)	15(3)
C4	86(4)	83(4)	59(4)	25(3)	25(3)	16(4)
C5	84(4)	69(4)	57(4)	5(3)	5(3)	-5(3)
C6	121(5)	99(5)	75(4)	13(4)	13(4)	6(4)
C7	115(5)	90(5)	76(4)	17(4)	17(4)	-1(4)
C8	157(6)	93(5)	76(4)	10(4)	10(4)	-3(4)
C9	214(8)	81(5)	70(4)	17(4)	17(4)	20(5)
C10	98(4)	68(4)	50(4)	11(3)	11(3)	6(3)
C11	103(5)	76(4)	50(4)	1(3)	1(3)	7(4)
C12	67(3)	60(4)	66(4)	4(3)	4(3)	-3(3)
C13	56(3)	47(3)	63(4)	13(3)	13(3)	11(3)

	U^{11}	U^{22}	U^{33}	U^{23}	U^{13}	U^{12}
C14	74(4)	75(4)	122(5)	19(4)	19(4)	-9(3)
C15	69(3)	70(4)	48(4)	17(3)	17(3)	0(3)
C16	63(3)	53(3)	44(4)	11(3)	11(3)	5(3)
C17	96(4)	98(5)	69(4)	13(3)	13(3)	-27(4)
C18	67(3)	55(3)	65(4)	6(3)	6(3)	6(3)
C19	59(3)	49(3)	59(4)	10(3)	10(3)	4(3)
C20	82(4)	78(4)	153(6)	39(4)	39(4)	35(4)

Table 5. Hydrogen coordinates ($x10^4$) and isotropic displacement parameters ($Å^2x10^3$) for am_k_09182015.

	x	y	z	U(eq)
H1A	1663	3400	8888	130
H1B	772	2240	9353	130
H1C	-355	2370	8336	130
H3	1199	3195	7281	83
H4	2613	3432	6014	89
H6	5188	2944	5004	114
H7	8169	961	5301	110
H8	9227	1280	3869	123
H9	7203	3865	4236	138

	x	y	z	U(eq)
H11	11715	4716	3882	94
H12	13205	5193	2684	79
H14A	13132	6083	1400	130
H14B	13588	5387	431	130
H14C	14781	4850	1326	130
H15	6872	2315	2173	72
H17A	6843	889	799	135
H17B	5984	1297	-174	135
H17C	5048	2037	687	135
H18	7031	587	6523	73
H20A	7113	-1317	7221	148
H20B	8033	-1268	8281	148
H20C	8891	-142	7781	148